Published in final edited form as:
Chem Res Toxicol. 2012 August 20; 25(8): 1682–1691. doi:10.1021/tx3001576.

Accurate and Efficient Bypass of 8,5'-Cyclopurine-2'-Deoxynucleosides by Human and Yeast DNA Polymerase η

Ashley L. Swanson[1], **Jianshuang Wang**[2], and **Yinsheng Wang**[1,2,*]

[1]Environmental Toxicology Graduate Program, University of California, Riverside, California 92521-0403

[2]Department of Chemistry, University of California, Riverside, California 92521-0403

Abstract

Reactive oxygen species (ROS), which can be produced during normal aerobic metabolism, can induce the formation of tandem DNA lesions, including 8,5'-cyclo-2'-deoxyadenosine (cyclo-dA) and 8,5'-cyclo-2'-deoxyguanosine (cyclo-dG). Previous studies have shown that cyclo-dA and cyclo-dG accumulate in cells and can block mammalian RNA polymerase II and replicative DNA polymerases. Here, we used primer extension and steady-state kinetic assays to examine the efficiency and fidelity for polymerase η to insert nucleotides opposite, and extend primer past, these cyclopurine lesions. We found that *Saccharomyces cerevisiae* and human polymerase η inserted 2'-deoxynucleotides opposite cyclo-dA, cyclo-dG, and their adjacent 5' nucleosides at fidelities and efficiencies that were similar as their respective undamaged nucleosides. Moreover, the yeast enzyme exhibited similar processivity in DNA synthesis on templates housing a cyclo-dA or cyclo-dG as those carrying an unmodified dA or dG; the human polymerase, however, dissociated from the primer-template complex after inserting one or two additional nucleotides after the lesion. Pol η's accurate and efficient bypass of cyclo-dA and cyclo-dG indicate that this polymerase is likely responsible for error-free bypass of these lesions, whereas mutagenic bypass of these lesions may involve other translesion synthesis DNA polymerases. Together, our results suggested that pol η may have an additional function in cells, i.e., to alleviate the cellular burden of endogenously induced DNA lesions, including cyclo-dA and cyclo-dG.

Introduction

Living cells are constantly exposed to a variety of endogenous and exogenous agents that can lead to DNA damage (1). One example is reactive oxygen species (ROS), which can be produced during normal aerobic metabolism. Aside from single-nucleobase lesions, ROS can give rise to the formation of tandem DNA lesions, including 8,5'-cyclo-2'-deoxyadenosine (cyclo-dA) and 8,5'-cyclo-2'-deoxyguanosine (cyclo-dG) (2). The cyclo-dA and cyclo-dG lesions can be detected at appreciable levels in DNA isolated from tissues of healthy animals without exposure to exogenous genotoxic agents (3–5). The cyclopurine lesions have a unique structure in that the C8 of the purine base is bonded with the C5' of 2-deoxyribose within the same nucleoside (Figure 1), which causes a distortion to DNA double helix and stabilization of *N*-glycosidic bond (6–8). A recent NMR structural study showed that, in duplex DNA, the 2-deoxyribose of (5'*S*)-cyclo-dG exhibits an O4'-exo conformation; although the modified nucleoside maintains Watson-Crick hydrogen-bonding interaction with the complementary cytosine base, the lesion introduces significant helical

*To whom correspondence should be addressed: yinsheng.wang@ucr.edu. Tel.: (951) 827-2700; Fax: (951) 827-4713..

Supporting Information Available: ESI-MS and MS/MS, primer extension, steady-state kinetic assay, and processivity results. This material is available free of charge via the Internet at http://pubs.acs.org.

and base stacking perturbations to the DNA duplex (9). Owing to these structural features, cyclo-dA and cyclo-dG block replicative DNA polymerases and mammalian RNA polymerase II, prevent their removal by base excision repair (BER), and subject them to nucleotide excision repair (NER) (5, 10–12). The endogenous accumulation of the cyclo-dA and cyclo-dG lesions may contribute to the development of cancer, neurodegeneration, and accelerated aging (4, 10, 13–15).

Translesion synthesis (TLS) is a damage tolerance pathway that facilitates replicative bypass of DNA lesions instead of repairing them (16, 17). This process utilizes specialized DNA polymerases, many of which belong to the Y-family, to insert nucleotides opposite and past the damage site (18, 19). These TLS polymerases often lack the efficiency and fidelity of traditional replicative polymerases because they have more spacious active sites, allowing them to accommodate bulky DNA lesions and erroneous base pairs (17). However, there are instances where TLS polymerases exhibit the ability to accurately and efficiently bypass certain DNA lesions (20–23). A striking example of this is polymerase η's capability in bypassing UV light-induced thymine-thymine cyclobutane pyrimidine dimer (CPD) with comparable efficiency and fidelity as that of an undamaged substrate (20, 24, 25). This is the main established role for pol η in cells, and the importance of which is manifested in those patients with XPV syndrome, as they lack a functional pol η and in turn display elevated mutagenesis and susceptibility in developing skin tumors (22, 26). However, this may not be pol η's sole role in cells, as this polymerase is capable of bypassing a wide array of DNA lesions with varying degrees of fidelity and efficiency (20, 25, 27, 28).

All Y-family polymerases have a little finger domain that is absent in replicative DNA polymerases, and when combined with the palm, thumb, and finger domains, can open the active site to allow for binding of modified nucleobases (17, 28, 29). However, pol η distinguishes itself from other Y-family polymerases in that the polymerase core is rotated away from the little finger, thereby creating an even larger binding pocket for accommodating two nucleotides into the active site (30, 31). Additionally, pol η has a distinct molecular splint that rigidly maintains the B-conformation of replicating DNA in the active site, minimizing the introduction of errors into the genome (28, 30, 31). The unique structure feature of pol η suggests that, apart from bypassing accurately CPD lesions, this polymerase may also be capable of handling other DNA lesions.

In the present study, we examined, by employing primer extension and steady-state kinetic assays, how site-specifically inserted cyclo-dA and cyclo-dG affect DNA replication mediated by *Saccharomyces cerevisiae* and human DNA pol η *in vitro*. We also assessed the processivity of these polymerases in bypassing the two purine cyclonucleosides. Our results suggest a new role for polymerase η in cells.

Materials and Methods

All unmodified oligodeoxyribonucleotides (ODNs) were purchased from Integrated DNA Technologies (Coralville, IA), and [γ-^{32}P]ATP was obtained from Perkin-Elmer (Boston, MA). *Saccharomyces cerevisiae* DNA polymerase η was expressed and purified following previously published procedures (32). Human DNA polymerase η was purchased from Enzymax (Lexington, KY). All other enzymes used in this study were from New England BioLabs (Ipswich, MA), and all chemicals were obtained from Sigma-Aldrich (St. Louis, MO).

Preparation of Lesion-bearing ODN Substrates

ODNs containing a cyclo-dA or cyclodG were previously synthesized (33). The identities of the 12mer lesion-bearing substrates were confirmed by electrospray ionization-mass

spectrometry (ESI-MS) and tandem mass spectrometry (MS/MS) analyses (21). The 12mer lesion-bearing substrates d(ATGGCGXGCTAT) [X = cyclo-dA or cyclo-dG] were ligated with a 5'-phosphorylated 8mer, d(GATCCTAG), in the presence of a 30mer template ODN, d(CCGCTCCCTAGGATCATAGCYCGCCATGCT) (Y = dT or dC), using previously published procedures (32). The resulting lesion-bearing 20mer substrates were purified using 20% denaturing polyacrylamide gel electrophoresis (PAGE). PAGE and LC-MS/MS were employed to confirm the purity and identity of the lesion-bearing substrates (LC-MS and MS/MS results are displayed in Figures S1&S2).

Primer Extension Assay

The 20mer lesion-bearing ODNs or their corresponding unmodified ODNs (0.05 μM) were annealed with a 5'-^{32}P-labeled 13mer primer (0.05 μM) to give substrates for primer extension and steady-state kinetic experiments. The primer extension reaction was carried out under standing-start conditions with the addition of a mixture of all four dNTPs (250 μM each), yeast or human pol η (concentrations indicated in Figures S3&S4), and a buffer containing 10 mM Tris-HCl (pH 7.5), 5 mM $MgCl_2$, and 7.5 mM dithiothreitol (DTT) at 37°C for 1 hr. The reaction was terminated with an equal volume of formamide gel-loading buffer (80% formamide, 10 mM EDTA, pH 8.0, 1 mg/mL xylene cyanol, and 1 mg/mL bromophenol blue). The products were resolved on 20% denaturing polyacrylamide gels with 8 M urea, and gel-band intensities were quantified using a Typhoon 9410 Variable Mode Imager (Amersham Biosciences Co.) and ImageQuant 5.2 Software (Amersham Biosciences Co.).

Processivity Assay

To determine the processivity of pol η, the ^{32}P-labeled primer-template complex (10 nM) was preincubated with yeast or human pol η (20 nM) at 25°C for 15 min in a buffer containing 25 mM Na_3PO_4 (pH 7.0), 5 mM DTT, 100 μg/mL bovine serum albumin, and 10% glycerol. The reaction was subsequently initiated with addition of excess amount of sonicated herring sperm DNA (1 mg/mL, Promega, Madison, WI) to serve as a trap, a mixture of all four dNTPs (250 μM each), and 5 mM $MgCl_2$. To demonstrate the effectiveness of the trap, yeast or human pol η was also preincubated with the herring sperm DNA together with primer-template complex prior to dNTP and $MgCl_2$ addition; the lack of DNA synthesis under such conditions indicated that the excess herring sperm DNA was able to trap all polymerase molecules (Figure S5). Reactions were terminated at 30, 60, and 120 sec by adding an equal volume of formamide gel-loading buffer, and analyzed on 20% denaturing polyacrylamide gels. Gel-band intensities were quantified with phosphorimager analysis as described above. The following equation was used to calculate the percentage of active polymerase molecules incorporating N^{th} nucleotides, with the intensity of the band at position 1 indicated by I_1, and intensity of the band at position N indicated by I_N (34):

$$\%\ \text{active polymerases at } N = \frac{(I_N + I_{N+1} + \ldots) \times 100\%}{(I_1 + I_2 + \ldots)}$$

The processivity for each deoxynucleotide incorporation (N) is then obtained by the following equation (34):

$$P_N = \frac{\%\ \text{active polymerases at } N+1}{\%\ \text{active polymerases at } N}$$

Steady-state Kinetic Measurements

Steady-state kinetic assays were carried out using previously described procedures (35). The aforementioned ^{32}P-labeled primer-template complex (50 nM) was incubated with yeast or human pol η (1.2 nM) at 37°C for 10 min in the presence of individual dNTPs at various concentrations (indicated in Figures 4–6 & S6–S8) and a buffer containing 10 mM Tris-HCl (pH 7.5), 5 mM $MgCl_2$, and 7.5 mM DTT. The reaction was terminated with an equal volume of formamide gel-loading buffer as described above. Extension products were separated using denaturing PAGE and gel band intensities of the primer and extension products were again quantified using a phosphorimager, as described above. The concentration of individual dNTP was optimized to allow for less than 20% nucleotide incorporation. The kinetic parameters for the incorporation of incorrect and correct nucleotides, V_{max} and K_m, were determined by plotting the observed rate of nucleotide incorporation (V_{obs}) as a function of dNTP concentration using Origin 6.0 Software (OriginLab) and fitting the data with a non-linear curve regression following the Michaelis-Menten equation (35). The k_{cat} values were calculated by dividing the calculated V_{max} with the concentration of pol η used. The efficiency of nucleotide incorporation was calculated by the ratio of k_{cat}/K_m, and the frequencies of incorrect nucleotide insertion (f_{inc}) and extension (f_{ext}) were determined based on the ratio of k_{cat}/K_m value obtained for the insertion of incorrect nucleotide over that for the correct nucleotide incorporation at the insertion and extension steps, respectively.

Results

To understand how cyclo-dA and cyclo-dG are bypassed by pol η *in vitro*, we prepared 20mer ODN substrates harboring a site-specifically inserted (5'*S*)-cyclo-dA or (5'*S*)-cyclo-dG, and verified the integrities of the lesion-containing ODNs with mass spectrometric analyses (Supporting Figures S1&S2). We then performed primer extension, processivity, and steady-state kinetic assays to determine the effects of these lesions on the accuracy and efficiency of DNA replication mediated by yeast and human pol η.

Primer Extension across (5'S)-Cyclo-dA and (5'S)-Cyclo-dG with Yeast and Human pol η

We first performed primer extension assays to evaluate the ability of yeast and human pol η to extend a 13mer primer in the presence of a 20mer template containing a cyclo-dA, cyclo-dG and their respective unmodified nucleosides at a defined site (Figures S3&S4). We found that, in the presence of all four dNTPs, yeast pol η can bypass successfully (5'*S*)-cyclo-dA and (5'*S*)-cyclo-dG, and generate full-length extension products (Figure S3). However, human pol η is more hindered by these lesions, which is reflected by the significant amount of unextended primer and stalled extension one nucleotide away from the 3' end of the initial primer (Figure S4). Additionally, the amount of full-length replication products is very low (~ 1%), indicating that these lesions confer a significant blocking effect on the human polymerase (Figure S4).

Processivity of Yeast and Human Pol η on the (5'S) Diastereomer of Cyclo-dA and Cyclo-dG, and the Corresponding Undamaged Substrates

We utilized a previously reported assay to assess the processivity of yeast and human pol η on nucleotide incorporation using the lesion-containing and undamaged templates (36). The assay allows for the measurement of the number of 2'-deoxynucleotides that the polymerase incorporates in a single DNA-binding event, where the presence of excess herring sperm DNA serves to trap all polymerase molecules dissociating from the DNA template. We calculated the percentage of pol η molecules that incorporate *N* nucleotides, where the percentage of active polymerase molecules incorporating at least one nucleotide was set at 100% (see Materials & Methods, Figures 2&3 and Supporting Figure S5). For the control

dA- and dG-containing substrates, 88% and 84% of human pol η molecules incorporated at least two nucleotides in the template, respectively, with the percentage of polymerase molecules dropping to 24% and 18% with seven nucleotide additions in the template (Figure 3). The decrease in the percentage of active polymerase molecules with each subsequent nucleotide addition is attributed to their dissociation from the template. The cyclo-dA- and cyclo-dG-containing templates had 81% and 75% of active enzyme molecules incorporating a minimum of two nucleotides, and 28% and 15% incorporating at least three nucleotides, respectively (Figure 3); no subsequent nucleotide additions were observed for cyclo-dA or cyclo-dG past the third nucleotide. By contrast, yeast pol η synthesized DNA with remarkably similar processivity past the cyclo-dA- and cyclo-dG-containing templates as their corresponding undamaged dA and dG. The percentages of active yeast pol η molecules at each nucleotide addition on the cyclo-dA- and cyclo-dG-containing templates resemble closely those for their respective control substrates (Figure 3).

We also calculated the processivity, P_N, for yeast and human pol η to insert each nucleotide past the damaged and the corresponding non-damaged sites. With human pol η, the average P_N values were 0.81±0.19, 0.78±0.20, 0.58±0.33, and 0.47±0.40 for substrates containing dA, dG, cyclo-dA, and cyclo-dG, respectively (Figure 3). Thus, human pol η-mediated DNA synthesis occurs at low processivity, and the processivity is further decreased significantly by the presence of the two lesions. With yeast pol η, the average P_N values for dA-, dG-, cyclo-dA-, and cyclo-dG-containing substrates were 0.83±0.19, 0.80±0.22, 0.80±0.21, and 0.76±0.23, respectively, indicating that DNA synthesis with yeast pol η also occurs with low processivity (Figure 3); nevertheless, the processivities for DNA synthesis with cyclo-dA- and cyclo-dG-containing substrates are very similar to those for the corresponding dA- and dG-containing substrates.

Steady-state Kinetic Analyses of Human Pol η-mediated Nucleotide Insertion opposite (5'S)-cyclo-dA and (5'S)-cyclo-dG

We next employed steady-state kinetic assays to measure the kinetic parameters for nucleotide insertion opposite the lesions, as well as their respective unmodified nucleosides (Figure 4). Human pol η predominantly incorporated the correct dTMP opposite cyclo-dA with high accuracy and efficiency. Misincorporation of dAMP, dCMP, and dGMP occurred at very low frequencies (1.0%, 0.38%, and 0.47%, respectively. Table 1). Importantly, the efficiency of dTMP insertion opposite cyclo-dA was similar as that of the control dA substrate, with the observed k_{cat}/K_m values being 85 and 140 $\mu M^{-1}min^{-1}$, respectively. Likewise, human pol η mainly incorporated the correct dCMP opposite cyclo-dG, with little misincorporation of dAMP (0.17%), dTMP (1.2%) and dGMP (0.0015%, Table 1). Human pol η also inserted the correct dCMP opposite cyclo-dG with comparable efficiency as that of the control substrate; the observed k_{cat}/K_m values for dCMP insertion opposite cyclo-dG and dG were 54 and 100 $\mu M^{-1}min^{-1}$, respectively.

Steady-state Kinetic Analyses of Human Pol η-mediated Extension past (5'S)-cyclo-dA and (5'S)-cyclo-dG

We next evaluated the ability of human pol η to extend past cyclo-dA and cyclo-dG and their respective undamaged substrates, again using steady-state kinetic assays to determine the efficiency and fidelity of nucleotide insertion opposite the downstream 5' nucleoside (Figures 5&S6). Based on the kinetic parameters for the insertion step, we used a 14mer primer with the correct dNTP being inserted opposite the lesions and their controls, as well as the most preferentially misincorporated dNTP opposite cyclo-dA and cyclo-dG (dAMP and dTMP, respectively). When the correct dT is paired with cyclo-dA, extension past the lesion is highly accurate, which was accompanied with very low frequencies of misincorporation of dAMP (1.5%), dGMP (0.67%), and dTMP (0.0067%) opposite dG

(Table 2). The extension is also moderately efficient, where the insertion of the correct dCMP occurred at an efficiency that is ~35% relative to the corresponding extension past the control dA**:**dT pair (Table 2). However, extension past the cyclo-dA**:**dA base pair is highly error-prone, with significant misincorporation of dTMP opposite the adjacent base (f_{ext} = 83%, Table 2). The efficiencies for extension past the mismatch and correct base pairs are also markedly different, with dCMP insertion past the cyclodA**:**dA mismatch occurring at a frequency that is ~0.5% of that for the insertion past the correct cyclo-dA**:**dT base pair (i.e., 0.11 vs. 21 μM^{-1} min^{-1}, Table 2).

Similar findings were made for cyclo-dG. When the correct dC was placed opposite cyclo-dG at the primer end, human pol η was able to extend the primer by inserting preferentially the correct dCMP opposite dG, the next nucleoside in the template, with misincorporations of dAMP, dTMP and dCMP occurring at frequencies of 1.5%, 0.88% and 0.68%, respectively. The efficiency for dCMP insertion was, however, lower (~28%) than that observed for corresponding dCMP insertion past the dG:dC pair (Table 2). When the cyclodG**:**dT mismatch is placed at the primer/template junction, human pol η, however, severely misincorporated dAMP (8300%), dGMP (130%), and dTMP (98%) opposite the next nucleoside (dG) though this occurred with extremely low efficiencies (Table 2). These results demonstrate that the presence of a misincorporated nucleotide opposite the lesion introduces errors and hinders human pol η in the extension step. Collectively, the above results revealed that human pol η-mediated nucleotide incorporation opposite the two purine cyclonucleosides and their adjacent 5' unmodified nucleoside were accurate, though the cumulative efficiencies for these two insertion steps were decreased by ~ 5 and 6 folds by the presence of cyclo-dA and cyclo-dG, respectively.

Steady-state Kinetic Analyses of Yeast pol η-mediated Nucleotide Insertion opposite (5'S)-cyclodA and (5'S)-cyclo-dG

Similar as what we observed for human pol η, yeast pol η again preferentially incorporated the correct dTMP opposite cyclo-dA, with relatively low frequencies of misincorporation of dAMP (2.3%), dGMP (0.053%), and dCMP (0.042%, Table 3, Figure S7). Similarly, yeast pol η inserted preferentially the correct dCMP opposite cyclo-dG, with ~7.2% misincorporation of dTMP and very low frequencies of misinsertion of dGMP (0.14%) or dAMP (0.99%, Table 3, Figure S8). Remarkably, insertion of the correct dTMP opposite cyclo-dA was about twice as efficient as dTMP incorporation opposite the unmodified dA (Table 3). Likewise, yeast pol η exhibited an enhanced ability to insert the correct dCMP opposite cyclo-dG relative to an unmodified dG; the observed k_{cat}/K_m values for dCMP insertion opposite cyclo-dG and dG were 84 and 53 $\mu M^{-1} min^{-1}$, respectively (Table 3).

Steady-state Kinetic Analyses of Yeast pol η-mediated Extension past (5'S)-cyclo-dA and (5'S)-cyclo-dG

Next we assessed the ability of yeast pol η to extend past the above-described lesions and their respective controls, and our results showed that the extension step followed a similar pattern as that seen with human pol η (Figure 6). For extension past cyclo-dA**:**dT base pair, the polymerase incorporated the correct dCMP opposite the template dG, with similar efficiency as that observed for dCMP insertion opposite the dG past dA**:**dT base pair. Misincorporation of dTMP, dAMP, and dGMP occurred at low frequencies (0.092%, 0.14%, and 1.3%, respectively, see Table 2). The observed k_{cat}/K_m for the cyclo-dA**:**dT pair was 39 $\mu M^{-1} min^{-1}$, which is only slightly lower than the 50 μM^{-1} min^{-1} observed for the control dA**:**dT base pair. On the other hand, the presence of a misincorporated dA nucleoside at the primer end led to significant frequencies of misincorporation of dAMP (23%), dGMP (1.3%), and dTMP (0.25%, Table 4) opposite the downstream dG in the template.

Nevertheless, the efficiency for incorporating the correct dCMP remained similar to the control, with the observed k_{cat}/K_m value being 33 μM^{-1} min^{-1}.

For the cyclo-dG**:**dC base pair, yeast pol η again incorporated preferentially the correct dCMP opposite the dG in the template, with misincorporations of dTMP, dGMP and dAMP occuring at frequencies of 4.2%, 0.12% and 0.14%, respectively (Table 4). Yeast pol η also inserted dCMP at the extension step with similar efficiency as dCMP incorporation opposite dG for the control dG**:**dC base pair (45 vs. 52 $\mu M^{-1}min^{-1}$, Table 4). On the other hand, with a cyclodG:dT base pair at the primer/template junction, extension past the lesion was hindered and inaccurate, with substantial misincorporations of dAMP (2.8%), dGMP (49%), and dTMP (0.47%, Table 4). The k_{cat}/K_m for dCMP insertion past the cyclo-dG**:**dT base pair was 16 μM^{-1} min^{-1}, significantly lower than the 52 μM^{-1} min^{-1} found for the control dG**:**dC base pair (Table 4). Together, the above results demonstrated that, similar to its human counterpart, yeast pol η is capable of inserting nucleotides opposite cyclo-dA, cyclo-dG, and their neighboring 5' nucleoside with high accuracy. Moreover, the cumulative efficiencies for these two insertion steps were 1.8- and 1.4-fold higher for substrates containing cyclo-dA and cyclo-dG than their corresponding unmodified substrates.

Discussion

The most striking finding made from the present study is that polymerase η is able to insert nucleotides opposite cyclo-dA and cyclo-dG, and their adjacent 5' unmodified nucleoside, with comparable efficiency and fidelity as their respective undamaged substrates. Remarkably, *Saccharomyces cerevisiae* pol η was able to insert the correct nucleotides opposite the lesions with greater efficiency than the corresponding insertions opposite the unmodified nucleosides (by ~2.3 and ~1.6 folds for cyclo-dA and cyclo-dG, respectively), though the yeast enzyme was slightly more error-prone than its human counterpart (Figure 7). Additionally, processivity of yeast pol η-mediated DNA synthesis on the damaged and the corresponding undamaged substrates was strikingly similar. The enzyme, however, exhibits relatively low processivity toward the undamaged substrates (Figure 3), which is consistent with previous findings (34, 37).

Insertion opposite the two lesions and their neighboring 5' undamaged nucleoside with human pol η was highly accurate, with misincorporation frequencies being under 1.5% in both steps. The efficiencies for nucleotide insertion opposite the two lesions, however, were lower than those for the corresponding undamaged substrates (Figure 7). Different from its yeast counterpart, human pol η is less processive in DNA synthesis past the two lesions than their respective control substrates (Figures 2&3). Although the steady-state kinetic results for human pol η-mediated nucleotide insertion opposite cyclo-dA, cyclo-dG, and their neighboring 5' nucleosides suggest relatively high efficiency in lesion bypass, processivity data indicate that the polymerase can only insert one or two additional nucleotides past the two lesions before dissociating from the primer-template complex. Thus, human pol η can efficiently insert nucleotides opposite cyclo-dA, cyclo-dG and their immediate 5' neighboring nucleoside before another polymerase takes over to continue with DNA synthesis (17).

The steady-state kinetic results resemble closely those found for pol η-mediated insertion and extension past the CPD lesion (20, 25). The high efficiency and accuracy of nucleotide insertion opposite the two purine cyclonucleosides and their neighboring 5' nucleosides may be attributed to the structural features of pol η. Among the Y-family polymerases, pol η is unique in that the polymerase core has a large binding pocket capable of accommodating two nucleotides into its active site (30, 31). In addition, pol η has a distinct molecular splint that rigidly maintains the B-conformation of replicating DNA in the active site, which

minimizes erroneous nucleotide incorporation (28, 30, 31). Future structural studies on complexes formed between pol η and duplex DNA substrates housing a cyclo-dA or cyclo-dG will provide further insights about how these lesions are recognized by the polymerase.

Previous studies revealed that cyclo-dA and cyclo-dG are both cytotoxic and mutagenic in *E. coli* cells (38, 39). A recent replication study showed that cyclo-dA and cyclo-dG strongly blocked DNA replication in AB1157 *E. coli* cells and produced mutations during replication, with cyclo-dA and cyclo-dG yielding A→T and G→A mutations at frequencies of 11% and 20%, respectively (38). This is in line with our observations that these lesions directed yeast and human polymerase η to misincorporate mainly dAMP opposite cyclo-dA and dTMP opposite cyclo-dG at low frequencies of ~2.3% and 1.0% (for cyclo-dA), and ~7.0% and 1.2% (for cyclodG), respectively. *E. coli* Pol V and eukaryotic pol η are considered orthologs because they exhibit similar patterns of dNTP insertion opposite many DNA lesions (29). Depletion of Pol V was found to result in compromised bypass of (5'*S*)-cyclo-dA and (5'*S*)-cyclo-dG in *E. coli* cells (38, 39). Taken together, our results imply that pol η is likely responsible for the error-free bypass of cyclo-dA and cyclo-dG, whereas other TLS polymerases may contribute to the mutagenic bypass of these lesions. Future replication studies will be needed for revealing how cyclo-dA and cyclo-dG are bypassed by other TLS polymerases, how these lesions compromise DNA replication and how pol η affects the bypass of these lesions in mammalian cells.

Cyclo-dA and cyclo-dG are present at relatively abundant levels in genomic DNA of mammalian cells and tissues (3–5, 13); thus, the failure to bypass these replication-blocking lesions may contribute to the pathogenesis of human diseases. The results from the present study provided direct biochemical evidence to support that both yeast and human pol η are capable of bypassing accurately and efficiently the oxidatively induced cyclo-dA and cyclo-dG lesions. In this vein, aerobic metabolism and the resulting generation of ROS are also conserved across evolution. Therefore, aside from its well-established function in tolerating UV light-induced CPD lesions, pol η perhaps also assumes an evolutionarily conserved role in cells' tolerance of purine cyclonucleosides that are induced endogenously from byproducts of aerobic metabolism.

Supplementary Material

Refer to Web version on PubMed Central for supplementary material.

Acknowledgments

Funding Support: This work was supported by the National Institutes of Health (R01 CA101864 to Y. W.) and Ashley L. Swanson was supported by an NRSA Institutional Training grant (T32 ES018827).

Abbreviations

ROS	Reactive oxygen species
cyclo-dA	8,5'-cyclo-2'-deoxyadenosine
cyclo-dG	8,5'-cyclo-2'-deoxyguanosine
BER	base excision repair
NER	nucleotide excision repair
TLS	translesion synthesis
ODN	oligodeoxyribonucleotide

PAGE	polyacrylamide gel electrophoresis
DTT	dithiothreitol

References

(1). Lindahl T. Instability and decay of the primary structure of DNA. Nature. 1993; 362:709–715. [PubMed: 8469282]

(2). Wang Y. Bulky DNA lesions induced by reactive oxygen species. Chem. Res. Toxicol. 2008; 21:276–281. [PubMed: 18189366]

(3). Tilstra JS, Robinson AR, Wang J, Gregg SQ, Clauson CL, Reay DP, Nasto LA, St Croix CM, Usas A, Vo N, Huard J, Clemens PR, Stolz DB, Guttridge DC, Watkins SC, Garinis GA, Wang Y, Niedernhofer LJ, Robbins PD. NF-κB inhibition delays DNA damage-induced senescence and aging in mice. J. Clin. Invest. 2012; 122 doi:10.1172/JCI45785.

(4). Wang J, Yuan B, Guerrero C, Bahde R, Gupta S, Wang Y. Quantification of oxidative DNA lesions in tissues of Long-Evans Cinnamon rats by capillary high-performance liquid chromatography-tandem mass spectrometry coupled with stable isotope-dilution method. Anal. Chem. 2011; 83:2201–2209. [PubMed: 21323344]

(5). Wang J, Clauson CL, Robbins PD, Niedernhofer LJ, Wang Y. The oxidative DNA lesions 8,5'-cyclopurines accumulate with aging in a tissue-specific manner. Aging Cell. 2012 DOI: 10.1111/j.1474-9726.2012.00828.x.

(6). Dizdaroglu M. Free-radical-induced formation of an 8,5'-cyclo-2'-deoxyguanosine moiety in deoxyribonucleic acid. Biochem. J. 1986; 238:247–254. [PubMed: 3800936]

(7). Jaruga P, Dizdaroglu M. 8,5'-Cyclopurine-2'-deoxynucleosides in DNA: mechanisms of formation, measurement, repair and biological effects. DNA Repair. 2008; 7:1413–1425. [PubMed: 18603018]

(8). Dizdaroglu M, Dirksen ML, Jiang HX, Robbins JH. Ionizing-radiation-induced damage in the DNA of cultured human cells. Identification of 8,5'-cyclo-2'-deoxyguanosine. Biochem. J. 1987; 241:929–932. [PubMed: 3496079]

(9). Huang H, Das RS, Basu AK, Stone MP. Structure of (5'*S*)-8,5'-cyclo-2'-deoxyguanosine in DNA. J. Am. Chem. Soc. 2011; 133:20357–20368. [PubMed: 22103478]

(10). Kuraoka I, Bender C, Romieu A, Cadet J, Wood RD, Lindahl T. Removal of oxygen free-radical-induced 5',8-purine cyclodeoxynucleosides from DNA by the nucleotide excision-repair pathway in human cells. Proc. Natl. Acad. Sci. USA. 2000; 97:3832–3837. [PubMed: 10759556]

(11). Jaruga P, Xiao Y, Vartanian V, Lloyd RS, Dizdaroglu M. Evidence for the involvement of DNA repair enzyme NEIL1 in nucleotide excision repair of (5'*R*)- and (5'*S*)-8,5'-cyclo-2'-deoxyadenosines. Biochemistry. 2010; 49:1053–1055. [PubMed: 20067321]

(12). Kuraoka I, Robins P, Masutani C, Hanaoka F, Gasparutto D, Cadet J, Wood RD, Lindahl T. Oxygen free radical damage to DNA. Translesion synthesis by human DNA polymerase η and resistance to exonuclease action at cyclopurine deoxynucleoside residues. J. Biol. Chem. 2001; 276:49283–49288. [PubMed: 11677235]

(13). Brooks PJ. The 8,5'-cyclopurine-2'-deoxynucleosides: candidate neurodegenerative DNA lesions in xeroderma pigmentosum, and unique probes of transcription and nucleotide excision repair. DNA Repair. 2008; 7:1168–1179. [PubMed: 18495558]

(14). Brooks PJ, Wise DS, Berry DA, Kosmoski JV, Smerdon MJ, Somers RL, Mackie H, Spoonde AY, Ackerman EJ, Coleman K, Tarone RE, Robbins JH. The oxidative DNA lesion 8,5'-(*S*)-cyclo-2'-deoxyadenosine is repaired by the nucleotide excision repair pathway and blocks gene expression in mammalian cells. J. Biol. Chem. 2000; 275:22355–22362. [PubMed: 10801836]

(15). Jaruga P, Dizdaroglu M. Identification and quantification of (5'*R*)- and (5'*S*)-8,5'-cyclo-2'-deoxyadenosines in human urine as putative biomarkers of oxidatively induced damage to DNA. Biochem. Biophys. Res. Commun. 2010; 397:48–52. [PubMed: 20471371]

(16). Sancar A, Lindsey-Boltz LA, Unsal-Kacmaz K, Linn S. Molecular mechanisms of mammalian DNA repair and the DNA damage checkpoints. Annu. Rev. Biochem. 2004; 73:39–85. [PubMed: 15189136]

(17). Lehmann AR, Niimi A, Brown S, Sabbioneda S, Wing JF, Kannouche PL, Green CM. Translesion synthesis: Y-family polymerases and the polymerase switch. DNA Repair. 2007; 6:891–899. [PubMed: 17363342]

(18). Lehmann AR. New functions for Y family polymerases. Mol. Cell. 2006; 24:493–495. [PubMed: 17188030]

(19). Prakash S, Prakash L. Translesion DNA synthesis in eukaryotes: a one- or two-polymerase affair. Genes Dev. 2002; 16:1872–1883. [PubMed: 12154119]

(20). Johnson RE, Prakash S, Prakash L. Efficient bypass of a thymine-thymine dimer by yeast DNA polymerase, Pol η. Science. 1999; 283:1001–1004. [PubMed: 9974380]

(21). Yuan B, Cao H, Jiang Y, Hong H, Wang Y. Efficient and accurate bypass of N^2-(1-carboxyethyl)-2'-deoxyguanosine by DinB DNA polymerase *in vitro* and *in vivo*. Proc. Natl. Acad. Sci. USA. 2008; 105:8679–8684. [PubMed: 18562283]

(22). Johnson RE, Kondratick CM, Prakash S, Prakash L. hRAD30 mutations in the variant form of xeroderma pigmentosum. Science. 1999; 285:263–265. [PubMed: 10398605]

(23). Jarosz DF, Godoy VG, Delaney JC, Essigmann JM, Walker GC. A single amino acid governs enhanced activity of DinB DNA polymerases on damaged templates. Nature. 2006; 439:225–228. [PubMed: 16407906]

(24). McCulloch SD, Kokoska RJ, Masutani C, Iwai S, Hanaoka F, Kunkel TA. Preferential cis-syn thymine dimer bypass by DNA polymerase η occurs with biased fidelity. Nature. 2004; 428:97–100. [PubMed: 14999287]

(25). Washington MT, Prakash L, Prakash S. Mechanism of nucleotide incorporation opposite a thymine-thymine dimer by yeast DNA polymerase eta. Proc. Natl. Acad. Sci. USA. 2003; 100:12093–12098. [PubMed: 14527996]

(26). Masutani C, Kusumoto R, Yamada A, Dohmae N, Yokoi M, Yuasa M, Araki M, Iwai S, Takio K, Hanaoka F. The XPV (xeroderma pigmentosum variant) gene encodes human DNA polymerase η. Nature. 1999; 399:700–704. [PubMed: 10385124]

(27). Carlson KD, Washington MT. Mechanism of efficient and accurate nucleotide incorporation opposite 7,8-dihydro-8-oxoguanine by *Saccharomyces cerevisiae* DNA polymerase η. Mol. Cell. Biol. 2005; 25:2169–2176. [PubMed: 15743815]

(28). Broyde S, Patel DJ. DNA repair: How to accurately bypass damage. Nature. 2010; 465:1023–1024. [PubMed: 20577203]

(29). Lee CH, Chandani S, Loechler EL. Homology modeling of four Y-family, lesion-bypass DNA polymerases: the case that *E. coli* Pol IV and human Pol κ are orthologs, and *E. coli* Pol V and human Pol η are orthologs. J. Mol. Graph Model. 2006; 25:87–102. [PubMed: 16386932]

(30). Silverstein TD, Johnson RE, Jain R, Prakash L, Prakash S, Aggarwal AK. Structural basis for the suppression of skin cancers by DNA polymerase η. Nature. 2010; 465:1039–1043. [PubMed: 20577207]

(31). Biertumpfel C, Zhao Y, Kondo Y, Ramon-Maiques S, Gregory M, Lee JY, Masutani C, Lehmann AR, Hanaoka F, Yang W. Structure and mechanism of human DNA polymerase η. Nature. 2010; 465:1044–1048. [PubMed: 20577208]

(32). Gu C, Wang Y. LC-MS/MS identification and yeast polymerase η bypass of a novel γ-irradiation-induced intrastrand cross-link lesion G[8–5]C. Biochemistry. 2004; 43:6745–6750. [PubMed: 15157108]

(33). Romieu A, Gasparutto D, Cadet J. Synthesis and characterization of oligonucleotides containing 5',8-cyclopurine 2'-deoxyribonucleosides: (5'*R*)-5',8-cyclo-2'-deoxyadenosine, (5'*S*)-5',8-cyclo-2'-deoxyguanosine, and (5'*R*)-5',8-cyclo-2'-deoxyguanosine. Chem. Res. Toxicol. 1999; 12:412–421. [PubMed: 10328751]

(34). Washington MT, Johnson RE, Prakash S, Prakash L. Fidelity and processivity of *Saccharomyces cerevisiae* DNA polymerase η. J. Biol. Chem. 1999; 274:36835–36838. [PubMed: 10601233]

(35). Goodman MF, Creighton S, Bloom LB, Petruska J. Biochemical basis of DNA replication fidelity. Crit. Rev. Biochem. Mol. Biol. 1993; 28:83–126. [PubMed: 8485987]

(36). von Hippel PH, Fairfield FR, Dolejsi MK. On the processivity of polymerases. Ann. N.Y. Acad. Sci. 1994; 726:118–131. [PubMed: 8092670]

(37). Washington MT, Johnson RE, Prakash S, Prakash L. Accuracy of thymine-thymine dimer bypass by *Saccharomyces cerevisiae* DNA polymerase η. Proc. Natl. Acad. Sci. USA. 2000; 97:3094–3099. [PubMed: 10725365]

(38). Yuan B, Wang J, Cao H, Sun R, Wang Y. High-throughput analysis of the mutagenic and cytotoxic properties of DNA lesions by next-generation sequencing. Nucleic Acids Res. 2011; 39:5945–5954. [PubMed: 21470959]

(39). Jasti VP, Das RS, Hilton BA, Weerasooriya S, Zou Y, Basu AK. (5'*S*)-8,5'-cyclo-2'-deoxyguanosine is a strong block to replication, a potent pol V-dependent mutagenic lesion, and is inefficiently repaired in *Escherichia coli*. Biochemistry. 2011; 50:3862–3865. [PubMed: 21491964]

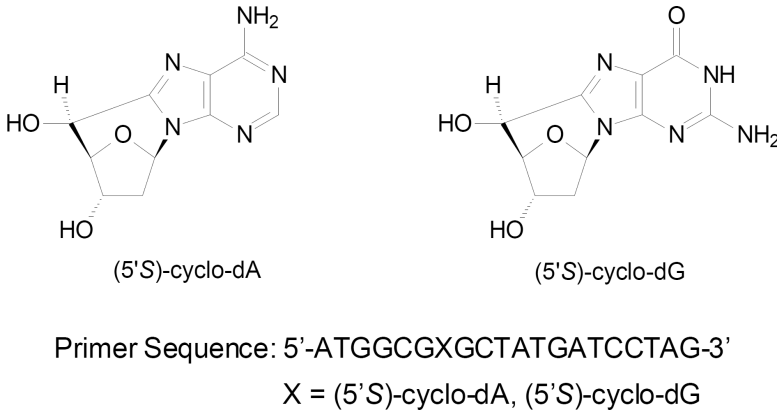

Figure 1.
Structures of the two cyclopurine lesions, (5'*S*)-cyclo-dA and (5'*S*)-cyclo-dG, as well as the 20mer sequences used for the *in vitro* replication studies.

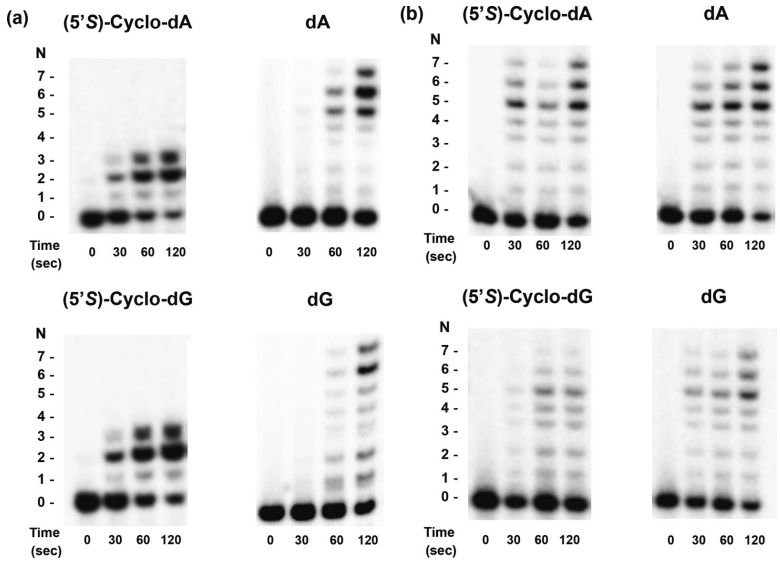

Figure 2.

Processivity assays for substrates containing (5'*S*)-cyclo-dA, (5'*S*)-cyclo-dG, dA, and dG, with human (a) and yeast pol η (b). The radiolabeled primer-template complex was preincubated with human pol η for 15 min. The reaction was then initiated with excess herring sperm DNA as a trap, all four dNTPs, and $MgCl_2$. Reactions were stopped at various time points indicated in the figures. The 120 sec time-point was used to calculate the percentage of active polymerase molecules and processivity values. Products were resolved on 20% denaturing polyacrylamide gels.

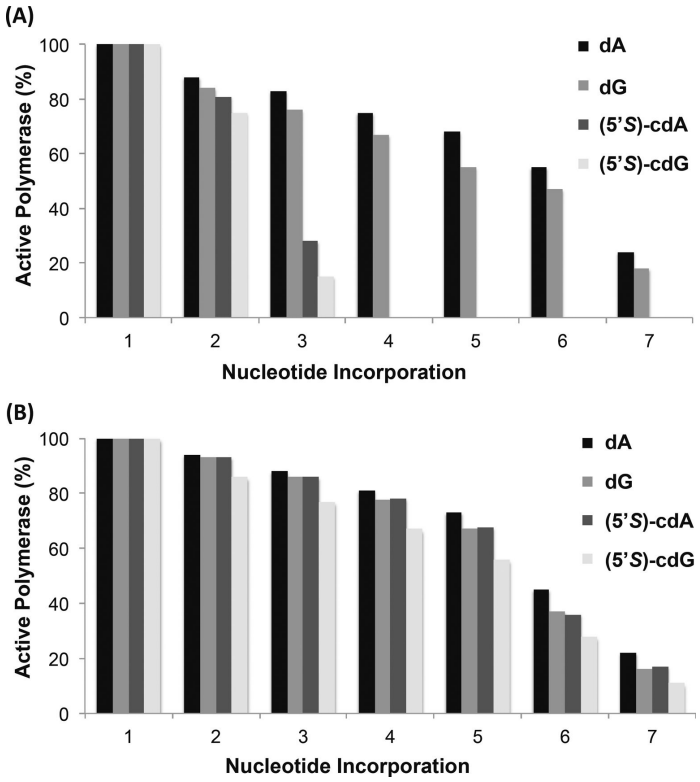

Figure 3.

Graphs depicting the percentage of active human polymerase η (a) or yeast polymerase η (b) molecules at each position along the template strand containing a site-specifically inserted (5'*S*)-cyclo-dA, (5'*S*)-cyclo-dG, dA, or dG (indicated in the legend).

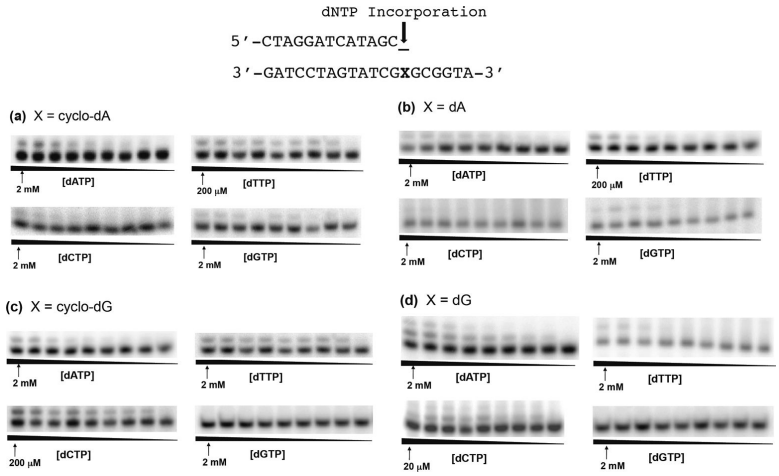

Figure 4.

Representative gel images for steady-state kinetic assays measuring nucleotide incorporation opposite (5′*S*)-cyclo-dA and (5′S)-cyclo-dG, and unmodified dA and dG. Reactions were carried out using 1.2 nM human pol η in the presence of individual dNTPs with the highest concentrations indicated in the figures. Concentration ratios between neighboring lanes were 0.50.

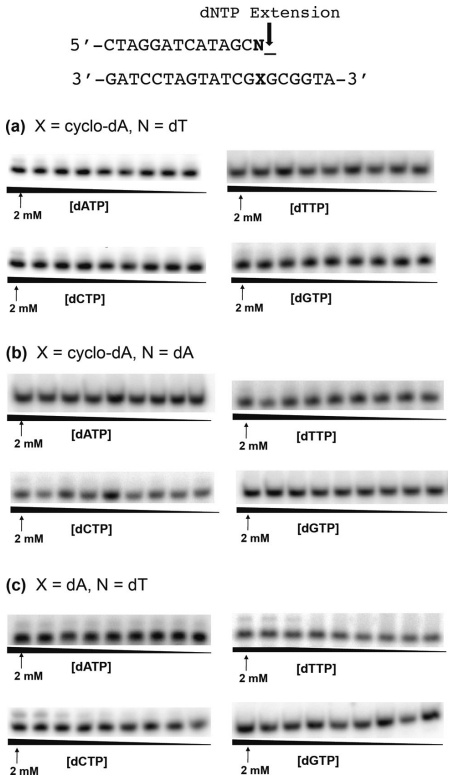

Figure 5.

Representative gel images for steady-state kinetic assays measuring extension past (5'*S*)-cyclo-dA and dA, with the base opposite the lesions indicated as `N'. Reactions were carried out using 1.2 nM human pol η in the presence of individual dNTPs with the highest concentrations indicated in the figures. Concentration ratios between neighboring lanes were 0.50.

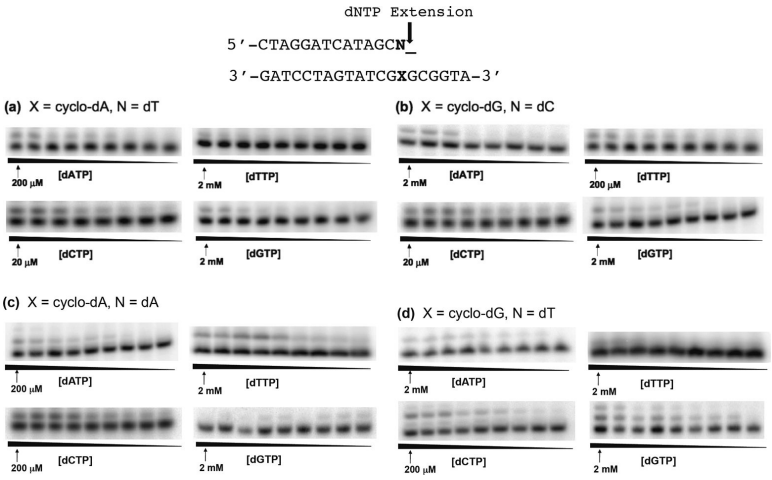

Figure 6.

Representative gel images for steady-state kinetic assays measuring extension past (5'*S*)-cyclo-dA (a,c) and (5'*S*)-cyclo-dG (b,d). Reactions were carried out using 1.2 nM yeast pol η in the presence of individual dNTPs with the highest concentrations indicated in the figures. Concentration ratios between neighboring lanes were 0.50.

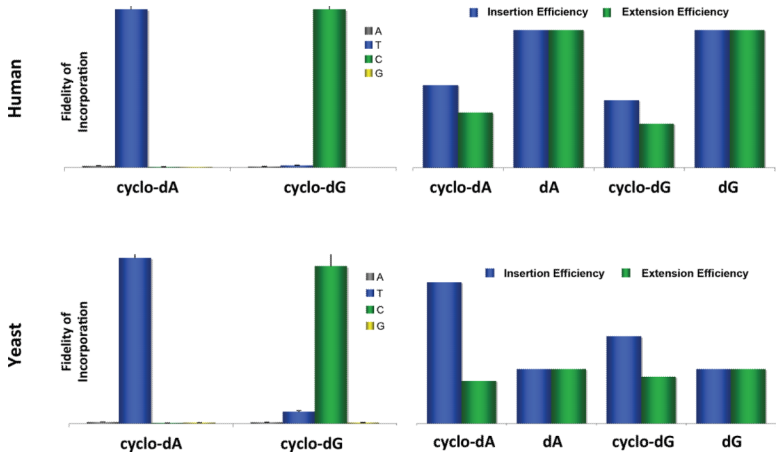

Figure 7.

Comparison of the fidelity of incorporation, incorporation efficiencies, and extension efficiencies mediated by human pol η and yeast pol η opposite and past (5'*S*)-cyclo-dA and (5'*S*)-cyclo-dG, and the undamaged nucleosides dA and dG.

Table 1

Steady-state Kinetic Parameters for Human pol η-mediated Nucleotide Insertion opposite Cyclo-dA and Cyclo-dG, and opposite Unmodified dA and dG[a]

dNTP	k_{cat} (min^{-1})	k_m (μM)	k_{cat}/K_m ($\mu M^{-1}min^{-1}$)	f_{inc}
(5'S)-cyclo-dA-containing substrate				
dTTP	11 ± 1	0.13 ± 0.01	85 ± 8	1
dGTP	6.4 ± 0.6	16 ± 1	0.41 ± 0.04	4.7×10^{-3}
dCTP	3.9 ± 0.2	12 ± 1	0.32 ± 0.03	3.8×10^{-3}
dATP	22 ± 2	26 ± 2	0.85 ± 0.09	1.0×10^{-2}
dA Control				
dTTP	18 ± 1	0.12 ± 0.01	140 ± 10	1
dGTP	11 ± 1	45 ± 4	0.25 ± 0.02	1.8×10^{-3}
dCTP	6.5 ± 0.6	13 ± 1	0.52 ± 0.05	3.7×10^{-3}
dATP	26 ± 2	24 ± 2	1.1 ± 0.01	7.8×10^{-3}
(5'S)-cyclo-dG-containing substrate				
dTTP	17 ± 1	28 ± 1	0.61 ± 0.06	1.2×10^{-2}
dGTP	0.71 ± 0.08	900 ± 100	0.00079 ± 0.00009	1.5×10^{-5}
dCTP	18 ± 1	0.36 ± 0.03	54 ± 6	1
dATP	16 ± 1	170 ± 15	0.094 ± 0.008	1.7×10^{-3}
dG Control				
dTTP	9.1 ± 0.9	48 ± 5	0.19 ± 0.01	1.9×10^{-3}
dGTP	1.0 ± 0.2	720 ± 90	0.0014 ± 0.0003	1.4×10^{-5}
dCTP	15 ± 1	0.13 ± 0.01	100 ± 10	1
dATP	31 ± 3	460 ± 50	0.067 ± 0.006	6.7×10^{-4}

[a] k_{cat} and K_m values were based on three independent measurements

Table 2

Steady-state Kinetic Parameters for Human pol η-mediated Extension past Cyclo-dA and Cyclo-dG, and Unmodified dA and dG (designated with an X, and N is the nucleoside placed opposite X)[a]

dNTP	k_{cat} (min^{-1})	K_m (μM)	k_{cat}/K_m ($\mu M^{-1}min^{-1}$)	f_{ext}
X = (5'S)-cyclo-dA, N = dT				
dTTP	0.93 ± 0.1	660 ± 80	0.0014 ± 0.0003	6.7×10^{-5}
dGTP	3.3 ± 0.3	28 ± 2	0.12 ± 0.01	5.7×10^{-3}
dCTP	6.3 ± 0.6	0.35 ± 0.03	21 ± 1	1
dATP	4.2 ± 0.4	15 ± 1	0.28 ± 0.01	1.3×10^{-2}
X = (5'S)-cyclo-dA, N = dA				
dTTP	3.8 ± 0.3	42 ± 4	0.091 ± 0.009	8.3×10^{-1}
dGTP	0.88 ± 0.1	710 ± 90	0.0012 ± 0.0002	1.1×10^{-2}
dCTP	3.9 ± 0.3	35 ± 3	0.11 ± 1	1
dATP	0.62 ± 0.09	850 ± 100	0.00073 ± 0.00009	6.6×10^{-3}
X = dA, N = dT				
dTTP	6.6 ± 0.6	19 ± 1	0.35 ± 0.03	5.9×10^{-3}
dGTP	0.77 ± 0.09	830 ± 90	0.00093 ± 0.0001	1.6×10^{-5}
dCTP	14 ± 1	0.24 ± 0.02	59 ± 5	1
dATP	6.4 ± 0.6	15 ± 1	0.43 ± 0.04	7.3×10^{-3}
X = (5'S)-cyclo-dG lesion-containing substrate, N = dC				
dTTP	4.7 ± 0.4	34 ± 3	0.14 ± 0.01	8.8×10^{-3}
dGTP	3.9 ± 0.4	38 ± 3	0.11 ± 0.01	6.8×10^{-3}
dCTP	7.4 ± 0.7	0.46 ± 0.04	16 ± 1	1
dATP	5.4 ± 0.5	23 ± 2	0.24 ± 0.02	1.5×10^{-2}
X = (5'S)-cyclo-dG lesion-containing substrate, N = dT				
dTTP	0.82 ± 0.1	840 ± 100	0.00098 ± 0.0002	9.8×10^{-1}
dGTP	0.93 ± 0.2	690 ± 80	0.0013 ± 0.0003	1.3
dCTP	0.89 ± 0.1	880 ± 100	0.0010 ± 0.0002	1
dATP	3.3 ± 0.3	39 ± 3	0.085 ± 0.008	85
X = dG, N = dC				
dTTP	9.6 ± 0.9	36 ± 3	0.27 ± 0.02	4.8×10^{-3}
dGTP	11 ± 1	24 ± 3	0.46 ± 0.04	8.2×10^{-3}
dCTP	12 ± 1	0.21 ± 0.02	56 ± 5	1
dATP	4.1 ± 0.4	19 ± 1	0.22 ± 0.02	3.9×10^{-3}

[a] k_{cat} and K_m values were based on three independent measurements

Table 3

Steady-state Kinetic Parameters for *S. cerevisiae* pol η-mediated Nucleotide Insertion opposite Cyclo-dA and Cyclo-dG, and opposite Unmodified dA and dG[a]

dNTP	k_{cat} (min^{-1})	K_m (μM)	k_{cat}/K_m ($\mu M^{-1}min^{-1}$)	f_{inc}
(5'S)-cyclo-dA-containing substrate				
dTTP	22 ± 1	0.14 ± 0.01	110 ± 10	1
dGTP	6.8 ± 0.3	130 ± 10	0.058 ± 0.005	5.3×10^{-4}
dCTP	5.4 ± 0.2	120 ± 10	0.046 ± 0.003	4.2×10^{-4}
dATP	16 ± 1	6.5 ± 0.4	2.5 ± 0.2	2.3×10^{-2}
dA Control				
dTTP	15 ± 1	0.31 ± 0.02	48 ± 4	1
dGTP	11 ± 0.5	210 ± 20	0.052 ± 0.003	1.1×10^{-3}
dCTP	40 ± 3	400 ± 30	0.089 ± 0.002	1.8×10^{-3}
dATP	10 ± 1	310 ± 13	0.033 ± 0.001	6.9×10^{-4}
(5'S)-cyclo-dG-containing substrate				
dTTP	17 ± 1	2.8 ± 0.2	6.1 ± 0.6	7.2×10^{-2}
dGTP	12 ± 1	95 ± 8	0.12 ± 0.01	1.4×10^{-3}
dCTP	21 ± 2	0.25 ± 0.01	84 ± 7	1
dATP	14 ± 1	17 ± 1	0.82 ± 0.07	9.9×10^{-3}
dG Control				
dTTP	18 ± 1	74 ± 6	0.24 ± 0.02	4.5×10^{-3}
dGTP	15 ± 1	520 ± 30	0.029 ± 0.001	5.5×10^{-4}
dCTP	27 ± 2	0.51 ± 0.04	53 ± 3	1
dATP	21 ± 2	110 ± 10	0.19 ± 0.01	3.6×10^{-3}

[a] k_{cat} and K_m values were based on three independent measurements

Table 4

Steady-state Kinetic Parameters for *S. cerevisiae* pol η-mediated Extension past Cyclo-dA and Cyclo-dG, and Unmodified dA and dG (designated with an X, and N is the nucleoside placed opposite X)[a]

dNTP	k_{cat} (min^{-1})	K_m (μM)	k_{cat}/K_m ($\mu M^{-1}min^{-1}$)	f_{ext}
X = (5'S)-cyclo-dA, N = dT				
dTTP	12 ± 1	330 ± 20	0.036 ± 0.002	9.2×10^{-4}
dGTP	14 ± 1	250 ± 20	0.056 ± 0.003	1.4×10^{-3}
dCTP	18 ± 1	0.46 ± 0.02	39 ± 3	1
dATP	17 ± 1	35 ± 5	0.49 ± 0.4	1.3×10^{-2}
X = (5'S)-cyclo-dA, N = dA				
dTTP	13 ± 1	160 ± 10	0.081 ± 0.007	2.5×10^{-3}
dGTP	12 ± 1	28 ± 2	0.43 ± 0.03	1.3×10^{-2}
dCTP	14 ± 1	0.42 ± 0.04	33 ± 1	1
dATP	13 ± 1	1.7 ± 0.1	7.6 ± 0.7	2.3×10^{-1}
X = dA, N = dT				
dTTP	19 ± 1	170 ± 10	0.011 ± 0.0009	2.2×10^{-4}
dGTP	13 ± 1	220 ± 10	0.057 ± 0.0052	1.1×10^{-3}
dCTP	30 ± 2	0.61 ± 0.03	50 ± 3	1
dATP	0.96 ± 0.2	660 ± 80	0.0014 ± 0.0002	2.8×10^{-5}
X = (5'S)-cyclo-dG, N = dC				
dTTP	19 ± 1	9.8 ± 0.7	1.9 ± 0.1	4.2×10^{-2}
dGTP	14 ± 1	250 ± 20	0.056 ± 0.004	1.2×10^{-3}
dCTP	22 ± 2	0.49 ± 0.04	45 ± 4	1
dATP	16 ± 1	250 ± 20	0.064 ± 0.005	1.4×10^{-3}
X = (5'S)-cyclo-dG, N = dT				
dTTP	12 ± 1	160 ± 10	0.075 ± 0.007	4.7×10^{-3}
dGTP	15 ± 1	1.9 ± 0.1	7.9 ± 0.6	4.9×10^{-1}
dCTP	15 ± 1	0.95 ± 0.04	16 ± 1	1
dATP	14 ± 1	31 ± 3	0.45 ± 0.04	2.8×10^{-2}
X = dG, N = dC				
dTTP	15 ± 1	270 ± 20	0.056 ± 0.005	1.1×10^{-3}
dGTP	11 ± 1	410 ± 35	0.027 ± 0.002	5.2×10^{-4}
dCTP	25 ± 2	0.48 ± 0.03	52 ± 4	1
dATP	14 ± 1	310 ± 15	0.045 ± 0.004	8.7×10^{-4}

[a] k_{cat} and K_m values were based on three independent measurements